19th International Conference
ENGINEERING MECHANICS 2013
Svratka, Czech Republic, May 13 – 16, 2013

# 2D FINITE ELEMENT ANALYSIS OF AGGREGATE INFLUENCE ON MECHANICAL PROPERTIES OF MORTAR SAMPLES

V. Nežerka, J. Vorel, J. Zeman [1]

**Abstract:** *Virtual testing of composite materials is, compared to a conventional experimental analysis, less time consuming, and it can very clearly reveal the failure mode. Therefore, it can be used for an optimization of the shape and amount of aggregates. Unlike the basic analytical homogenization methods, numerical modeling can predict the strength of the material and energy needed for the crack propagation. In our study three-point bending and splitting tests, by means of 2D plane-stress nonlinear finite element analysis utilizing isotropic damage model, were simulated. The results of the analysis indicate that angular aggregates of bigger size contribute to an increased fracture energy of the mortars, while the mortars containing fine round aggregates exhibit higher strength due to absence of stress concentrations around the grains.*

**Keywords:** ***FEM, damage model, mortar, influence of aggregates***

## 1. Introduction

It has been observed by many researchers (e.g. Stefanidou and Papayianni (2005); Tasong et al. (1998)) that the material properties of mortars and concrete are dependent on the amount, type and geometry of aggregates in the mix. The purpose of this work was to investigate the influence of the aggregate shape and size on the mechanical properties of mortars, composed of sand aggregates and a brittle matrix. Namely, the influence of aggregates on flexural strength of the tested mortar was determined from a three-point bending test simulations, while the fracture energy was evaluated from simulations of a splitting test.

Commonly used homogenization methods, such as the Mori-Tanaka scheme (Mori and Tanaka (1973); Benveniste (1987)), can quite successfully predict the elasticity properties, but they are not able to predict the strength and to capture the post-peak behavior of the composite materials. Such properties must be estimated numerically, using the Finite Element Modeling. Among others, Vorel et al. (2012) have recently estimated the fracture energy of concrete using 2D plane-stress model of three-point bending test on notched specimens, the fracture energy of concrete was also investigated by van Mier and van Vliet (2003) using 2D lattice model. and similar approach was used by Man and van Mier (2011). Finally, Mohamed and Hansen (1999) simulated the interaction of crack and aggregate during splitting test using 2D plane-stress model.

## 2. Geometry of Tested Specimens

The simulations were focused on the investigation of aggregate shape and size influence on

[1] Ing. Václav Nežerka, Doc. Ing. Jan Zeman, Ph.D., Ing. Jan Vorel, Ph.D., Faculty of Civil Engineering, Czech Technical University in Prague, Thákurova 7, 166 29 Praha 6, Czech Republic; e-mail: vaclav.nezerka@fsv.cvut.cz

the bending strength evaluated from three-point bending tests, and fracture-mechanical properties evaluated from a series of splitting tests. In order to avoid the influence of size effects (Jueshi and Hui (1997); Zhang and Wu (1999)) on the values of fracture energy, all specimens were of the same size. The geometry of tested specimens is specified by Figures 1a and 1b.

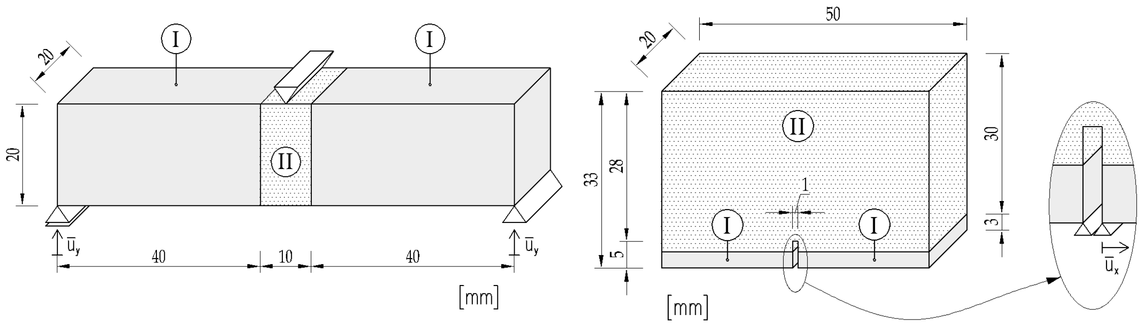


(a) bending test

(b) splitting test

Figure 1: Geometry of tested specimens

The aggregates of round, ellipsoidal and angular shape were placed only in the area of expected crack propagation in a relative volume $c^{\mathrm{agg}} = 0.4$. Each aggregate shape configuration was represented by the fine (F) (passing the sieve opening $d_0$ = 1.0 mm) and coarse (C) ($d_0$ = 2.5 mm) monodisperse particles. The individual aggregate configurations are summarized in Table 1.

Table 1: Summary of simulated aggregate configurations

| | code | shorter semi-axis [mm] | longer semi-axis [mm] |
|---|---|---|---|
| angular coarse aggregates | A(C) | 2.5 | 5.0 |
| angular fine aggregates | A(F) | 1.0 | 2.0 |
| ellipsoidal coarse aggregates | E(C) | 2.5 | 5.0 |
| ellipsoidal fine aggregates | E(F) | 1.0 | 2.0 |
| round coarse aggregates | R(C) | 2.5 | 2.5 |
| round fine aggregates | R(F) | 1.0 | 1.0 |

## 3. Model

The procedure of the geometry generation was implemented in MATLAB software and the multi-parametric toolbox for MATLAB (Kvasnica (2009)) was used for the generation of the aggregates. The specimens were modeled as if they were cast into the final shape, i.e. the aggregates did not cross their boundaries. The conforming triangular finite element mesh was generated with the ANSYS software. Figure 2 shows the mesh density, which was coarse near supports in case three-point bending test and significantly finer in the expected crack location. This figure also depicts the crack propagation through the material.

The plane-stress numerical simulations were carried out in the OOFEM finite element code with the object oriented architecture (Patzák and Bittnar (2001)). An isotropic damage model

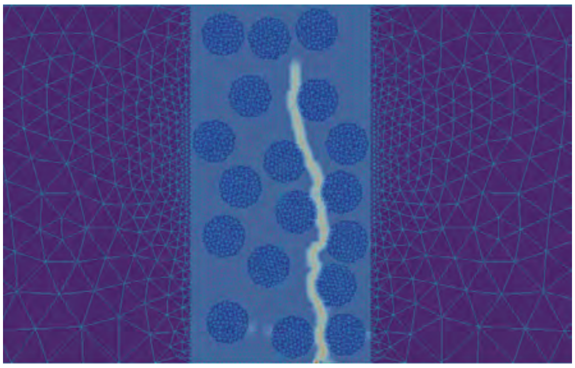

(a) bending test (configuration R(C))

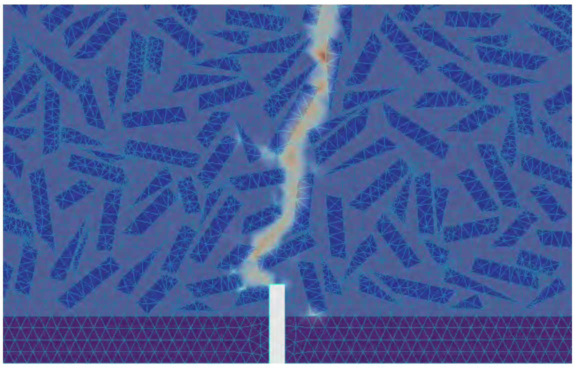

(b) splitting test (configuration A(C))

Figure 2: Detail of FE mesh and crack pattern

with linear softening (Jirásek (2004)) was assumed for the matrix phase, while the aggregates were modeled as isotropic and elastic. The equivalent strain, $\tilde{\varepsilon}$, was determined based on Mazars norm, accounting only for the positive part of the strain tensor. The interfacial transition zone was not modeled. The material properties of the matrix and aggregates are summarized in Table 2. The input parameters were: Young's modulus, $E$, Poisson's ratio, $\nu$, and in case of matrix also strain at peak stress $\varepsilon_0$ and crack opening at complete failure $w_{\mathrm{f}}$. In order to avoid damage around nodes with controlled displacement, the loaded and supported areas were also modeled as isotropic elastic material, having the stiffness of the homogenized material (denoted "homogenized regions" in Table 2) characterized by elastic constants obtained using Mori-Tanaka scheme (see Mori and Tanaka (1973); Benveniste (1987)).

Table 2: Material properties of individual phases

| | $E$ [GPa] | $\nu$ [-] | $\varepsilon_0$ [-] | $w_{\mathrm{f}}$ [µm] | note |
|---|---|---|---|---|---|
| matrix | 3.2 | 0.2 | 0.0004 | 1.0 | brittle material, linear softening |
| aggregates | 60.0 | 0.2 | - | - | elastic material |
| homogenized regions | 9.0 | 0.2 | - | - | elastic material |

The matrix phase was represented by a brittle lime-based paste and its properties were determined from our own experiments Nežerka et al. (2013), while the properties of aggregates were determined based on the literature study (Sharpe Jr. et al. (2007); Vorel et al. (2012)).

## 4. Results and Discussion

Six random distributions per each of the six different aggregate shape and size configurations were generated in order to obtain reliable data. The results were averaged within the individual configurations, providing a smooth force-displacement diagram. The averaging of forces at each displacement step was not possible, since such approach would yield unrealistic average curve, attaining the maximum value (force) of the "weakest" specimen. Therefore, the average curve was assembled in such a way to follow the mean elastic modulus and mean ultimate force reached during the loading. The softening part had to obey the mean value of the energy dissipated during the simulations, and it was approximated by a linear (three-point bending) or exponential curve (splitting test), see Figures 3a and 3b.

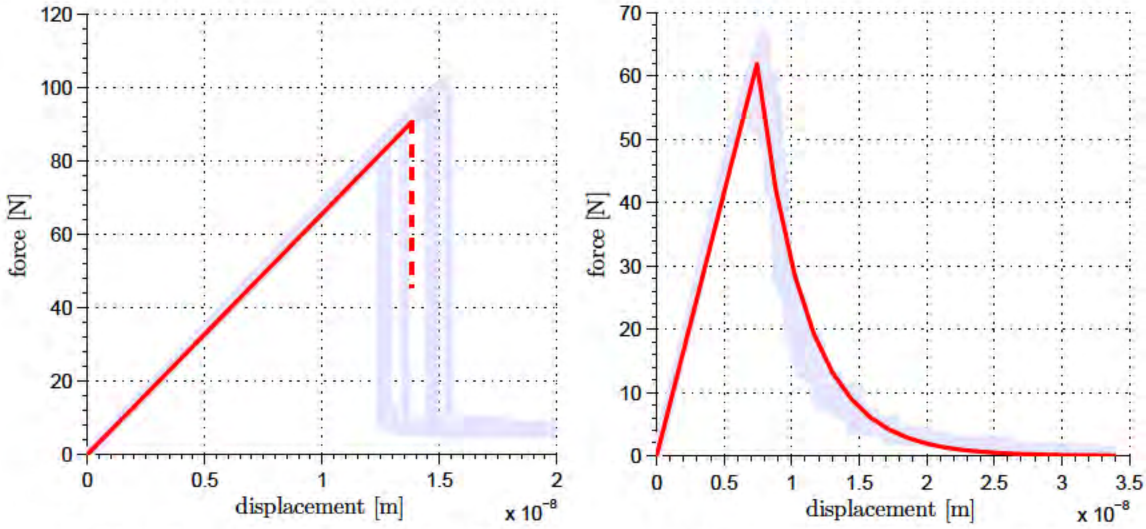


(a) bending test (configuration E(C)) (b) splitting test (configuration R(F))

Figure 3: Averaging of individual simulations within single configuration

The stress concentrations due to presence of angular particles resulted in a lower resistance of the specimens in three-point bending tests (see Figure 4a), which was even more pronounced in case of beams containing coarse particles. On the other hand, the fine round particles resulted in the highest bending strength. The stiffness of the specimens was not significantly influenced by the shape of the particles and the slight deviations were caused by the variable arrangement of the the particles within the sample.

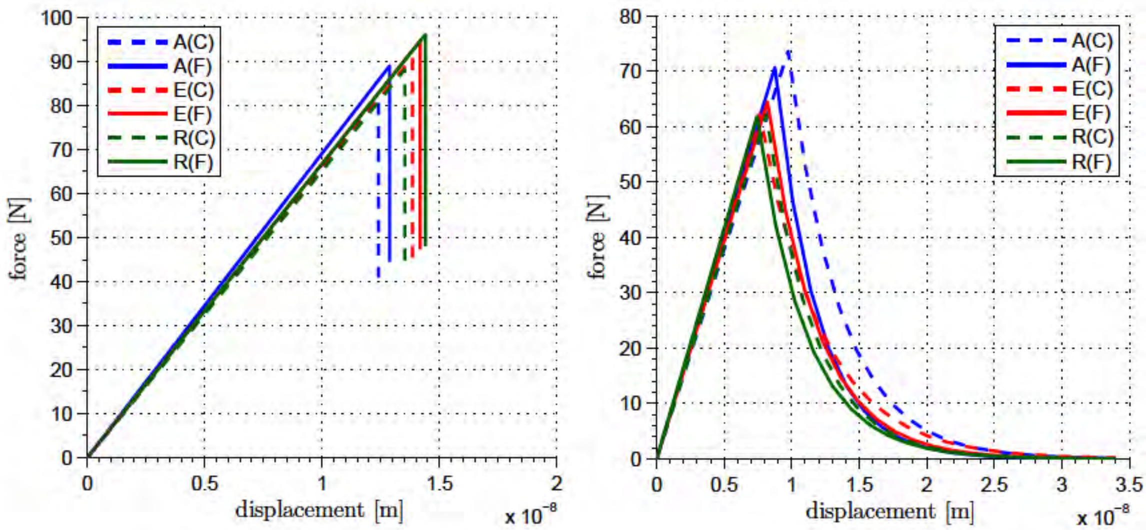


(a) bending test (b) splitting test

Figure 4: Averaged load-displacement diagrams for individual aggregate configurations

The opposite trends were observed in splitting simulations (see Figure 4b), where the coarse angular aggregates contributed to higher fracture energy of the mortar, while the round aggregates enabled relatively easy crack propagation through the specimens. The results of the simulations are summarized in Tables 3 and 4. The work of fracture in the splitting test was calculated as the area under the loading curve of the load-displacement diagrams.

Table 3: Results of three-point bending test simulations

| configuration | maximum force $F_{\max}$ [N] | displacement at $F_{\max}$ [$\times 10^{-9}$ m] |
|---|---|---|
| A(C) | 81.9 | 1.24 |
| A(F) | 89.0 | 1.29 |
| E(C) | 90.9 | 1.38 |
| E(F) | 94.7 | 1.42 |
| R(C) | 88.1 | 1.35 |
| R(F) | 96.1 | 1.44 |

Table 4: Results of splitting test simulations

| configuration | maximum force $F_{\max}$ [N] | displacement at $F_{\max}$ [$\times 10^{-9}$ m] | work of fracture [$\times 10^{-7}$ J] |
|---|---|---|---|
| A(C) | 73.6 | 9.74 | 6.43 |
| A(F) | 69.6 | 9.28 | 5.46 |
| E(C) | 62.3 | 7.63 | 5.25 |
| E(F) | 64.5 | 8.21 | 5.04 |
| R(C) | 62.1 | 8.11 | 4.74 |
| R(F) | 61.9 | 7.43 | 4.56 |

## 5. Conclusions

The present work was focused on the influence of aggregates embedded in the brittle matrix, represented by the isotropic damage model with linear softening. In particular, the bending strength and fracture-mechanical properties were evaluated from the finite element simulations of bending and splitting tests. The following conclusions can be made from the results of the analysis:

- 2D plane-stress finite element simulations and isotropic damage model can successfully simulate the crack propagation through a microstructure in a realistic way,
- simulation of splitting test can be used for the evaluation of fracture energy in brittle materials without snap-back response in load-displacement diagram,
- the bending strength is enhanced by the addition of fine spherical sand particles into mortars, since they do not introduce excessive stress concentrations around their tips,
- the fracture energy of mortars can be enhanced by the addition of coarse angular aggregates, since these create an efficient obstacle against the crack propagation.

The study was not supposed to yield exact values, it only revealed the trends. Three-dimensional model, incorporating shrinkage microcracking and interfacial zone around aggregates, would probably give more accurate data at significantly higher computational cost.

**Acknowledgment**

The authors would like to thank for the financial support by the grant no. SGS13/034/OHK1/1T/11.

**References**

Benveniste, Y. (1987). A new approach to the application of Mori-Tanaka theory in composite materials. *Mechanics of Materials*, 6:147–157.

Jirásek, M. (2004). Non-local damage mechanics with application to concrete. *Revue Europeaenne de Génie Civil*, 8:683–707.

Jueshi, Q. and Hui, L. (1997). Size effect on fracture energy of concrete determined by three-point bending. *Cement and Concrete Research*, 27:1031–1036.

Kvasnica, M. (2009). *Real-Time Model Predictive Control via Multi-Parametric Programming: Theory and Tools*. VDM Verlag, Saarbruecken.

Man, H.-K. and van Mier, J. (2011). Damage distribution and size effect in numerical concrete from lattice analyses. *Cement & Concrete Composites*, 33:867–880.

Mohamed, A. and Hansen, W. (1999). Micromechanical modeling of crack-aggregate interaction in concrete materials. *Cement & Concrete Composites*, 21:349–359.

Mori, T. and Tanaka, K. (1973). Average stress in matrix and average elastic energy of materials with mixfitting inclusions. *Acta Metallurgica*, 21:571–574.

Nežerka, V., Slížková, Z., Tesárek, P., Plachý, T., Frankeová, D., and Petráňová, V. (*submitted 2013*). Comprehensive study on microstructure and mechanical properties of lime-pozzolan pastes. *Cement and Concrete Research*.

Patzák, B. and Bittnar, Z. (2001). Design of object oriented finite element code. *Advances in Engineering Software*, 32:759–767.

Sharpe Jr., W., Pulskamp, J., Gianola, D., Eberl, C., Polcawich, R., and Thompson, R. (2007). Strain Measurements of Silicon Dioxide Microspecimens by Digital Imaging Processing. *Experimental Mechanics*, 47:649–658.

Stefanidou, M. and Papayianni, I. (2005). The role of aggregates on the structure and properties of lime mortars. *Cement & Concrete Composites*, 27:914–919.

Tasong, W., Lynsdale, C., and Cripps, J. (1998). Aggregate-cement paste interface: influence of aggregate physical properties. *Cement and Concrete Research*, 28(10):1453–1465.

van Mier, J. and van Vliet, M. (2003). Influence of microstructure of concrete on size/scale effects in tensile fracture. *Engineering Fracture Mechanics*, 70:2281–2306.

Vorel, J., Šmilauer, V., and Bittnar, Z. (2012). Multiscale simulations of concrete mechanical tests. *Journal of Computational and Applied Mathematics*, 236:4882–4892.

Zhang, D. and Wu, K. (1999). Fracture process zone of notched three-point-bending concrete beams. *Cement and Concrete Research*, 29:1887–1892.